Modifications of perineuronal nets and remodelling of excitatory and inhibitory afferents during vestibular compensation in the adult mouse

Brain Structure and Function, 221(6): 3193-3209*, 2016*
DOI: 10.1007/s00429-015-1095-7

Modifications of perineuronal nets and remodelling of excitatory and inhibitory afferents during vestibular compensation in the adult mouse

Faralli Alessio[1,2], Dagna Federico[3], Albera Andrea[1,2], Oohashi Toshi[4], Albera Roberto[3], Rossi Ferdinando[1,2†] and Carulli Daniela[1,2]

[1] Department of Neuroscience, Neuroscience Institute of Turin (NIT), University of Turin, Regione Gonzole 10, 10043 Orbassano (Turin), Italy
[2] Neuroscience Institute of the Cavalieri-Ottolenghi Foundation (NICO), University of Turin, Regione Gonzole 10, 10043 Orbassano (Turin), Italy
[3] Department of Surgical Sciences, University of Turin, Via Genova 3, 10100 Turin, Italy
[4] Department of Molecular Biology and Biochemistry, Okayama University Graduate School of Medicine, Dentistry and Pharmaceutical Sciences, Okayama 700-8558, Japan
[†] In memoriam

Corresponding author

Daniela Carulli

Neuroscience Institute of the Cavalieri-Ottolenghi Foundation (NICO)

University of Turin

Regione Gonzole 10

10043 Orbassano (Turin)

Italy

Phone: +39-011-6706614

Fax: +39-011-6706621

E-mail: daniela.carulli@unito.it

Abstract

Perineuronal nets are aggregates of extracellular matrix molecules surrounding several types of neurons in the adult CNS, which contribute to stabilising neuronal connections. Interestingly, in conditions associated with plasticity in the adult brain, a reduction of PNNs has been observed. However, it is not known whether PNN changes are functional to plasticity and repair after injury. To address this issue we investigated PNN expression and anatomical remodelling in the vestibular nuclei of the adult mouse during vestibular compensation. Vestibular compensation refers to the resolution of postural and oculomotor deficits resulting from a peripheral vestibular lesion. We found that following unilateral labyrinthectomy, static postural functions of the mouse recuperate in 2 weeks, while dynamic reflexes in 4 weeks. Remarkable structural plasticity of glutamatergic and GABAergic fibres was observed in the lateral vestibular nucleus on both sides at different time points after unilateral labyrinthectomy, which may contribute to functional recovery. Moreover, PNNs appeared strongly attenuated during the course of vestibular symptoms amelioration, while they were completely restored once vestibular deficits had fully recovered. Interestingly, in mice with genetically defective PNNs vestibular compensation was accelerated. Overall, these results indicate that plasticity mechanisms underlying vestibular compensation depend crucially on PNN modulation.

Keywords

Plasticity, vestibular compensation, labyrinthectomy, perineuronal nets, vestibular nuclei, Bral2.

Highlights

- Vestibular compensation in the adult mouse occurs within 4 weeks.
- Vestibular compensation is accompanied by axonal remodelling in vestibular nuclei.
- Perineuronal nets are attenuated during amelioration of vestibular deficits.
- Perineuronal nets are restored once vestibular symptoms have completely resolved.
- In mice with reduced perineuronal nets vestibular compensation is accelerated.

Introduction

The PNN is a layer of condensed extracellular matrix which enwraps the soma and proximal dendrites of several types of neuron in the adult CNS, with holes at sites of synaptic contacts. The main components of PNNs are hyaluronan, link proteins, chondroitin sulphate proteoglycans (CSPGs), semaphorin3A and tenascin-R (Köppe et al., 1997; Carulli et al., 2007; Kwok et al., 2010; Vo et al., 2013). CSPGs in the extracellular space interact with hyaluronan on the cell surface, and this interaction is stabilized by the presence of link proteins (Kwok et al., 2011). PNNs are formed at the end of developmental critical periods for experience-dependent plasticity and contribute to the stabilisation of specific connection patterns, thus limiting plasticity (Wang and Fawcett, 2012; Geissler et al., 2013). Pharmacological degradation of PNNs in the adult CNS restores juvenile levels of plasticity and enhances cognitive functions (Pizzorusso et al., 2002, 2006; Gogolla et al., 2009; Romberg et al., 2013; Happel et al., 2014; Yang et al,. 2014). Mutant mice with vestigial PNNs (due to the lack of the PNN component cartilage link protein-1) show persistent plasticity into adulthood and enhanced memory (Carulli et al., 2010; Romberg et al., 2013). Interestingly, in several conditions associated with plasticity in the adult brain, a reduction in PNNs has been observed. For example, exposure to an enriched environment induces significant axonal changes in the cerebellar nuclei, which are accompanied by a conspicuous reduction of PNNs (Foscarin et al., 2011). Environmental enrichment also increases visual cortex plasticity in the adult, in parallel with reduced density of PNNs (Sale et al., 2007). PNNs are also diminished during enhanced neuritic remodelling after injury (Carmichael et al., 2005; Carulli et al., 2013).

Understanding cellular and molecular events regulating structural plasticity is crucial to promote functional recovery after CNS damage or correct developmentally miswired neuronal connections. Vestibular compensation is an attractive model of deafferentation-induced plasticity in the adult brain. The vestibular system is a sensory system concerned with the sensation of head position and movement and the generation of reflexes for stabilising gaze and body posture. Unilateral damage to the vestibular peripheral receptors and nerve peripheral terminals (i.e. labyrinthectomy) causes progressive degenerative changes of vestibular nerve fibres, inducing a partial and gradual deafferentation of the vestibular nuclei (VN) (Gacek and Schoonmaker, 1997; Lacour et al., 2009). Neurons of deafferented VN lose their normal high resting activity, while those of the contralateral side become hyperactive. The consequent asymmetry of the resting discharge between the intact and deafferented VN is believed to cause the severe oculomotor and postural symptoms that immediately follow the damage, e.g. vertigo, spontaneous ocular nystagmus, postural instability (Lacour and Tighilet, 2010). In most species, the static syndrome (i.e. symptoms continuously

present even in totally stationary subjects) largely disappears in a few days (Vidal et al., 1998). The initial rapid stage of vestibular compensation is followed by a slower process in which dynamic deficits (which manifest as a result of head motion in space) recover, although in some cases never completely (Vibert et al., 1993; Gliddon et al., 2005). Since in mammals there is no regeneration of the lesioned labyrinth or the vestibular nerve, vestibular compensation is attributed to functional and structural plasticity in the VN, cerebellum and related structures (Curthoys and Halmagyi, 1999). VN are composed of four main nuclei, the superior, lateral (LVN), medial and inferior (Highstein and McCrea, 1988; see for review Grassi and Pettorossi, 2001). Previous reports showed reactive neurogenesis and gliogenesis in the denervated VN (De Waele et al., 1996; Campos-Torres et al., 1999, 2005; Tighilet et al., 2007; Lacour et al., 2009), which play a role in functional recovery through the activity of $GABA_A$ receptors (Dutheil et al., 2009, 2013). Moreover, BDNF upregulation, along with its TrKB receptor, is found bilaterally in the LVN after UL and may contribute to vestibular compensation (Smith et al. 1998; Lacour and Tighilet, 2010). Significant changes in the expression of choline acetyltransferase, GABA, neuroprotective factors, markers of inflammatory response and extracellular matrix molecules (Liberge et al., 2010, Gustave-Dit-Duflo et al., 1999; Tighilet and Lacour, 1998, 2001; Deák et al,. 2012) have also been detected in the VN after peripheral damage.

In the present study we investigated whether: i) the expression of PNNs in the LVN of the adult mouse is altered during compensation of vestibular static and dynamic deficits, in parallel with enhanced structural plasticity; ii) vestibular compensation is affected in mice with genetically defective PNNs.

Material and methods

Experimental animals

The experiments were performed on 3 month-old FVB, C57BL/6 mice (Harlan, San Pietro al Natisone, Italy) and homozygous Bral2 knock-out (KO) mice (Bekku et al., 2012). Pax2-GFP transgenic mice were used to visualize GABAergic interneurons (Bouchard et al., 2005). Animals were maintained on a 12 h light/dark cycle at a constant temperature (22°C) with ad libitum access to food and water. All procedures were in accordance with the European Communities Council Directive (2010/63/EU), the NIH guidelines and the Italian Law for Care and Use of Experimental Animals (DL26/14) and were approved by the Italian Ministry of Health and the Bioethical Committee of the University of Turin. Every attempt was made to minimize the number and the suffering of animals used in these experiments.

Unilateral labyrinthectomy (UL)

Mice were anaesthesized by intraperitoneal administration of ketamine (100 mg/kg; Ketavet, Bayer) supplemented by xylazine (5 mg/kg; Rompun, Bayer). A skin incision was performed behind the external acoustic meatus of the right ear. The tympanic membrane, malleus, incus, and stapes were removed. The ventral wall of the tympanic bulla was carefully opened and the labyrinth containing the vestibular sense organs was mechanically destroyed and aspirated using a suction tube. The stapedial artery and the facial nerve were maintained intact.

Behavioural tests

Analysis of support surface

For behavioural tests, 6 female FVB mice, 11 C57Bl/6 mice and 15 Bral2 KOs were analysed.

The measure of the support surface, namely the surface delimited by the four paws of the mouse while standing erect at rest, allows to evaluate the postural stability of the animal. Support surface is a very sensitive parameter used for evaluating static posture deficit and recovery after a vestibular lesion (Liberge et al., 2010; Dutheil et al., 2013). Mice were placed in a box equipped with a transparent bottom and filmed from under this box. The support surface was measured by Image J software (Research Service Branch). Five repeated measurements were taken for each mouse at pre-operative time and at each post-operative time (1, 2, 3, 6, 8, 13, 16, 20, 24, 28, 48 days post-operation, dpo, for FVB mice; 1, 3, 7, 14, 21, 28, 35 dpo for C57Bl/6 and Bral2 KO mice), and the average for each time point was calculated. To compare C57Bl/6 and Bral2 KO mice, data collected after vestibular lesion were compared with pre-lesion values and expressed as percentage of the pre-op value.

Landing and air-righting

Dynamic postural deficits and recovery were evaluated in the same group of mice (n = 6) using two dynamic reflex tests, the air-righting reflex and the landing reflex.

The air-righting reflex was used to test the mouse ability to right itself in the air, while the landing reflex was used to test the response of the mouse to a vertical linear acceleration. During the air-righting test, the mouse was held at approximately 40 cm above a cushion, in supine position. The experimenter removed his/her hands as quickly and simultaneously as possible. In a normal mouse, just after the drop, the vestibular system detects a change in linear acceleration that triggers the head turning, which in turn induces the sequence of body repositioning. After vestibular lesion, the righting response is usually partially or totally abolished and it recovers with time through the

vestibular compensation process. A score of “0” was assigned when the air-righting reflex was complete, “2” when the animal failed to turn itself and fell on its back, and “1” when it showed a partial reaction and thus fell on its side.

During the landing reflex, the mouse was held by the base of the tail and lowered toward the ground. Animals with intact vestibular function flex their neck and extend their forelimbs as they approach the surface, whereas mice with vestibular lesion at an uncompensated stage show the right response only when their forepaws or vibrissae touch the ground. A score of“0” was assigned when the animals responded properly, and“2” if ground contact was required.

The scores for the air-righting reflex and the landing reflex were summed, providing a global score of dynamic vestibular function and recovery. A “0” score indicated a normal vestibular function, as observed before the vestibular lesion. Scores ranging from “1” to “4” indicate incomplete vestibular compensation.

Three repeated measurements were taken for each mouse before UL and at each postoperative time. A mean was calculated for the pre-operative time and for each post-lesion time (1, 2, 3, 6, 8, 13, 16, 20, 24, 28, 48 dpo). As for the support surface evaluation, each animal acted as its own control.

Histological procedures

Animals were anaesthetized and transcardially perfused with 100 ml of 4% paraformaldehyde in 0.12 M phosphate buffer. Brains were dissected and postfixed overnight at 4°C, then cryoprotected in 0.12 M phosphate buffer containing 30% sucrose at 4°C, until they sank. Brainstems were cut on a cryostat into 25 µm-thick coronal sections and collected in phosphate-buffered saline (PBS).

Primary antibodies were incubated overnight at room temperature (RT) in PBS containing 0.25% Triton X-100, and 1.5% serum of the species of the second antibody. They were the following: mouse anti-NeuN (Millipore, 1:500), to stain LVN neurons; mouse SMI32 (Sternberger/Covance Europe, 1:500), to stain LVN projection neurons; chicken anti-GFP (Aves, 1:700), to stain interneurons in Pax2-GFP mice; rabbit anti-VGLUT1 (Synaptic Systems, 1:1500) and guinea pig anti-VGLUT2 (Synaptic Systems, 1:1000), to stain glutamatergic terminals; guinea pig anti-VGAT (Synaptic Systems, 1:700), to stain GABAergic terminals; rabbit anti-brevican [kind gift of C. Seidenbecher (Leibniz Institute for Neurobiology, Magdeburg), 1:2000] to stain the PNN component brevican. To visualize PNNs, sections were incubated in biotinylated *Wisteria floribunda* agglutinin (WFA; Sigma Aldrich, 20 µg/ml) for 2 h at RT. Subsequently, sections were incubated for 1 h at RT with one of the following fluorophore-conjugated secondary antibodies: streptavidin Texas Red (Vector), goat anti-chicken Alexa Fluor 488 (Invitrogen), donkey anti-

mouse or anti-rabbit Alexa Fluor 488 (Invitrogen), donkey anti-rabbit Alexa Fluor 647 (Invitrogen), donkey anti-guinea pig Cy3 (Jackson Laboratories). After processing, sections were mounted on microscope slides with Tris-glycerol supplemented with 10% Mowiol (Calbiochem, LaJolla, CA). Histological preparations were examined under a E-800 Nikon microscope connected to a color CCD Camera, a Leica SP5 confocal microscope or a Nikon C1 confocal microscope. Confocal images were taken at a resolution of 1024x1024 dpi and 100 Hz speed and each focal plane was 1 µm-thick. Lasers intensity, gain and offset were maintained constant in each analysis. Quantitative and morphometric evaluations were made using the software Image J. Adobe Photoshop 6.0 (Adobe Systems, San Jose, CA) was used to adjust image contrast and assemble the final plates.

Morphometric evaluations of glutamatergic and GABAergic terminals

All the evaluations were performed in the ventral LVN, as the dorsal LVN is known to be devoid of vestibular nerve endings (Sotelo and Palay, 1970) and thus may not be directly affected by UL. To estimate the density of VGLUT1-, VGLUT2- and VGAT-positive axon terminals, we selected at least three sections containing the ventral LVN for each animal (FVB mice, 3-6 animals/each time point), and captured one 1-µm-thick confocal images/section under a 63x objective. On such images, which represented an area of 56,259 μm^2, we used the "analyze particle" function of ImageJ to estimate the number of boutons in the LVN on both sides. The density was expressed as number of terminals/mm^2. The "analyze particle" function of ImageJ was also used to evaluate the size of VGLUT1- and VGLUT2-positive axon terminals in the acquired images of control and 12 dpo-LVN.

Quantification of PNNs

Quantification of the number and staining intensity of PNNs was performed as in Foscarin et al. (2011). Briefly, the number of neurons bearing a PNN in the LVN on both sides was determined on sections which were double labelled with NeuN antibodies and WFA histochemistry. WFA is a general PNN marker, which binds to sugar chains of the CSPGs (Hartig et al., 1992). In each confocal image (acquired under a 63x objective), we sampled all the NeuN-positive neurons and calculated the percentage of neurons surrounded by a PNN (3 sections/mouse, 3-5 mice/time point). To compare different percentages, we transformed the values in radiants according to the arcsin transformation.

Analysis of WFA staining intensity was performed on confocal images collected under a 63x objective. By ImageJ, we measured the brightness intensity (range 0-255) of at least 30

PNNs/animal (3-6 mice/time point) by randomly selecting 15 pixels in the net and calculating their average. The background brightness, taken from a non-stained region of the cerebellar molecular layer, was subtracted from the brightness measurements. Each net was assigned to one of three categories of staining intensity, ranging from the lowest to the highest value of WFA intensity: weak = 0-33%, medium = 34-66%, strong = 67-100% of maximum staining intensity.

Statistical analysis

Statistical analyses were carried out by GraphPad Prism 5 (GraphPad Software Inc., La Jolla, CA, USA) and included Student's t-test, one-way ANOVA test followed by Dunnett's *post hoc* analysis and Chi-square test. In all instances, $P < 0.05$ was considered as statistically significant. Data were expressed as averages $\pm$ standard error of the mean (SEM).

Results

Recovery of postural vestibular functions in the adult mouse after unilateral labyrinthectomy

Typical signs of vestibular damage, such as head tilt, postural asymmetry and circling behaviour, were apparent when the mice recovered from anaesthesia. To analyse the time course of functional recovery of postural vestibular deficits, we evaluated: i) static posture functions, by measuring the surface delimited by the four paws of the mouse standing erect at rest (support surface) at different time points following UL (1, 2, 3, 6, 8, 13, 16, 20, 24, 28, 48 dpo); ii) dynamic posture functions, by testing the air-righting and landing reflexes of the mice at different time points after UL (see above). The support surface of the mice was strongly increased at 1 dpo (pre-op: 7.00 ± 0.17 cm^2; 1 dpo: 11.92 ± 1.04 cm^2; $P<0.001$ compared to pre-op value; **Fig. 1A**), due to the hyperextension of the contralateral hindlimbs. During the following days, the support surface progressively decreased, with a return to pre-operative values at 13 dpo (8.59 ± 0.65 cm^2; $P>0.05$; **Fig. 1A**).

Before UL, all mice showed a normal air-righting reflex (i.e. they were able to right themselves when held in a supine position and then dropped in the air), as well as a normal landing reflex (i.e. they extended their forelimbs when moved towards the ground held by the tail). The global score was, therefore, 0. After UL, the mice showed profound impairments in both tests, reaching the maximum global score at 1 dpo (3.50 ± 0.22; $P<0.001$ compared to pre-op score; **Fig. 1B**). A progressive recovery of dynamic reflexes occurred with time, thus the global score gradually decreased, reaching values similar to pre-op conditions at 24 dpo (0.92 ± 0.45; $P>0.05$; **Fig. 1B**).

Structural plasticity in the lateral vestibular nuclei after UL

To address whether vestibular compensation is accompanied by structural plasticity in the vestibular nuclei, we analysed the density of glutamatergic and GABAergic synaptic terminals in the ipsilateral and the contralateral ventral LVN at different time points after UL. GABAergic terminals, which may belong to local interneurons, commissural fibres, cerebellar nuclei neurons and Purkinje cells (Balaban et al., 2000; Holstein et al., 1999), were stained by anti-VGAT antibodies. Glutamatergic terminals, namely vestibular fibre endings (Zhang et al., 2010) as well as several other types of VN afferents (see discussion), were revealed by anti-VGLUT1 or VGLUT2 antibodies. Double labelling for VGLUT1 and VGLUT2 showed three types of glutamatergic axon terminals in the LVN: VGLUT1 single-labelled, VGLUT2 single-labelled and VGLUT1/VGLUT2 double-labelled, with a ratio of 1:83:16 (**Fig. 2A, B**). Thus, VGLUT1-positive boutons mainly represented a subpopulation of VGLUT2-positive terminals. VGLUT1-immunoreactive boutons

were on average of larger size than VGLUT2-positive ones (3.34 μm^2 ± 0.08 versus 2.66 μm^2 ± 0.04; P<0.001; **Fig. 2A, C**).

Ipsilateral side

When examining plasticity of glutamatergic axons in the ipsilateral LVN during vestibular compensation, we found that UL resulted in a progressive decrease in the density of glutamatergic terminals, which was particularly clear within the population of VGLUT1-positive terminals. In the first two weeks following UL, VGLUT1-terminals density decreased from 1164.02 ± 53.80 to 618.31 ± 72.77 at 3 dpo (47% decrease; P<0.001), 415.09 ± 52.38 at 6 dpo (64% decrease; P<0.001) and 224.33 ± 20.28 at 12 dpo (81% decrease; P<0.001; **Fig. 3A-D, P**). VGLUT2-positive terminals also decreased during vestibular compensation, although to a lesser extent than VGLUT1 terminals (3 dpo: from 7779.21 ± 283.84 to 6423.43 ± 539.77; 17% decrease, P<0.05; 6 dpo: 5992.66 ± 519.06; 23% decrease, P<0.01; 12 dpo: 5871.43 ± 128.03; 25% decrease, P<0.001; **Fig. 3F-I, Q**). As reported by Gacek and Schoonmaker (1997), reduced number of glutamatergic boutons may reflect vestibular nerve degeneration. Since glutamatergic terminals containing VGLUT1 appear strongly affected by UL, we expected that the average size of glutamatergic terminals in the LVN (which for the vast majority were VGLUT2-positive) was decreased. Indeed, VGLUT2-terminal average size at 12 dpo showed a 12% decrease when compared to control conditions (from 2.66 μm^2 ± 0.04 to 2.34 μm^2 ± 0.03; P<0.001; **suppl. Fig. 1A-C**). Interestingly, functional recovery at 24 dpo was accompanied by a substantial increase of glutamatergic boutons. Indeed, VGLUT1 boutons density showed an almost 800% increase with respect to the 12 dpo value, and a 49% increase when compared to control values (1735.91 ± 121.00; P<0.001; **Fig. 3E, P**); VGLUT2 density returned to control levels (7007.00 ± 457.75; P>0.05; **Fig. 3J, Q**).

To examine whether unilateral UL also induces plasticity of GABAergic axons in the ipsilateral LVN, we analysed the density of VGAT-terminals during vestibular compensation. The density of VGAT-positive terminals was 3522.19 ± 293.40 (**Fig. 3K, R**). No significant difference in the density of GABAergic terminals was detected at any time point post-lesion (P>0.05 compared to control values; **Fig. 3K-O, R**).

Contralateral side

Following UL, cellular and molecular changes have been reported in the contralateral VN (Gacek and Schoonmaker, 1997; Smith et al., 1998; Gustave-Dit-Duflo et al., 1999; Li et al., 2002; Liberge et al., 2010; Tighilet and Lacour, 1998, 2001, 2010). Therefore, we asked whether vestibular compensation was accompanied by structural plasticity also in the contralateral LVN. Interestingly, while the number of VGLUT2-terminals did not change at any time point after UL (P>0.05; **Fig.**

4F-J, Q), the number of VGLUT1-terminals showed a 75% increase at 24 dpo (from 1164.02 ± 53.80 to 2038.09 ± 109.62; P<0.001 compared to control LVN; **Fig. 4A-E, P**). Moreover, we found that VGAT-positive terminals were substantially increased in number at 6, 12 and 24 dpo (approximately 65% increase, from 3456.33 ± 283.41 to 5671.42 ± 258.78 at 6 dpo; P<0.001 with respect to intact LVN; 5079.95 ± 203.68; P<0.001 at 12 dpo; 5144.39 ± 195.46; P<0.001 at 24 dpo; **Fig. 4K-O, R**).

In summary, vestibular compensation was accompanied by considerable axonal remodelling in both the ipsilateral and the contralateral LVN. Namely, recovery of static deficits was associated with an increased density of GABAergic boutons in the contralateral LVN, while compensation of dynamic deficits was additionally accompanied by a dramatic increase in glutamatergic terminals in both LVN, which was particularly significant in the ipsilateral LVN.

PNNs in the LVN are reduced at early time points after UL and are restored when vestibular deficits have recovered

Previous works show prominent PNNs in the VN, composed of CSPGs (including aggrecan, versican, neurocan, brevican and phosphacan), hyaluronan, link proteins and semaphorin3A (Bruckner et al., 2000; Bekku et al., 2012; Vo et al., 2013; Rácz et al., 2014). We found numerous WFA-positive PNNs in the intact ventral LVN, which enwrapped projection neurons (87% of cases) and interneurons (SMI32-negative; 13% of cases) (**Fig. 5A-D**). Moreover, the vast majority of SMI32-positive neurons (98%) bore a PNN. Among those neurons, around 40% were GABAergic (revealed by GFP fluorescence in Pax2-GFP transgenic mice), suggesting that the remaining 60% of PNN-bearing SMI32-positive-neurons were glutamatergic (**Fig. 5A-C, E**). Furthermore, approximately 60% of all GABAergic neurons possessed a net (of which 67% were projection neurons; **Fig. 5A-C, F**).

To ask whether the observed local neuritic remodelling in the LVN of UL-mice is associated with permissive microenvironmental conditions generated by the lesion, we analysed whether PNNs were reduced after UL. First, we evaluated whether the number of neurons bearing a WFA-positive PNN changed during vestibular compensation. Notably, in the ipsilateral LVN, the number of PNN-bearing neurons dropped from 65.76% ± 2.20 to 20.04% ± 3.30 (P<0.001; **Fig. 6A-B', F**). The percentage of neurons with nets then increased progressively with time, becoming 39.89% ± 3.10 at 6 dpo (P<0.001 when compared to intact LVN; **Fig. 6C, C', F**), and returning to control levels from 12 dpo (P>0.05 with respect to intact LVN; **Fig. 6D-F**). We observed PNN changes also in the contralateral LVN, although to a lesser extent than in the ipsilateral LVN. Here, the number of

neurons with nets slightly decreased at 3 dpo (being 48.70% ± 2.23; P<0.001 with respect to intact LVN, **Fig. 7A-B', F**), and returned to control levels from 6 dpo (P>0.05; **Fig. 7C-F**).

To further characterize deafferentation-dependent modifications of the PNN structure, we divided the sampled nets in three categories according to the intensity of WFA staining (weakly, medium and strongly stained nets). Analysis of the relative distribution frequencies in these categories in intact conditions showed that weak nets were 8%, medium nets were 39% and strong nets were 53% (**Fig. 6G, 7G**). In the first 2 weeks after UL, a dramatic weakening of PNN labelling was apparent, particularly in the ispilateral LVN (**Fig. 6A-D', G** and **suppl. Fig. 2A, B**). Here, the percentage of weakly stained nets significantly increased when compared to intact conditions, being 56% at 3 dpo, 83% at 6 dpo and 78% at 12 dpo, while the frequency of strongly stained PNNs decreased (14% at 3 dpo, 1% at 6 dpo, 0% at 12 dpo) (X^2 test: P<0.001; **Fig. 6A-D', G**). Intriguingly, after 24 days the number of weak, medium and strong PNNs was comparable to the intact condition (X^2 test: P>0.05; **Fig. 6E, E', G**).

In the contralateral LVN, we also observed a significant progressive reduction in PNN staining intensity until 6 dpo (X^2 test: P<0.001; **Fig. 7A-D', G)**, then an increase at 12 dpo, with a complete recovery at 24 dpo (X^2 test between intact and 24 dpo: P>0.05; **Fig. 7E, E', G**). However, these changes were less substantial than those found in the ispilateral side (X^2 test: P<0.001 between ipsi- and contralateral LVN at each time point).

In summary, PNN are greatly reduced during vestibular compensation, particularly in the denervated LVN. PNN number is then restored in coincidence with compensation of static deficits, while PNN thickness returns to control levels when also dynamic functions are recovered.

Vestibular compensation is accelerated in Bral2 KO mice

Enzymatic digestion or genetic attenuation of PNNs are known to promote structural plasticity in the adult brain, ameliorate cognitive abilities and restore plasticity levels typical of critical periods (Pizzorusso et al., 2002, 2006; Carulli et al., 2010; Gogolla et al., 2009; Romberg et al., 2013; Happel et al., 2014; Yang et al., 2014). To elucidate whether UL-induced PNN reduction in the LVN is crucial for recovery of vestibular functions, we analysed vestibular compensation in a mouse model showing defective PNNs, due to the lack of Bral2. Bral2, together with cartilage link protein-1, is a link protein found in PNNs (Bekku et al., 2003, 2012). Bral2 knockout mice display attenuated WFA-bearing PNNs as well as a strong reduction of the PNN component brevican in several nuclei of the brainstem including the LVN (Bekku et al., 2012; **Fig. 8A-D**). To assess whether the presence of vestigial PNNs in Bral2 knockout mice affects vestibular compensation, we

examined postural static reflexes of Bral2 KOs and their WT counterpart (C57Bl/6 mice) at different time points after UL (1, 3, 7, 14, 21, 28, 35 dpo). UL caused a significant increase in the support surface of both C57Bl/6 mice and Bral2 KOs at 1 dpo (approximately 20% increase; **Fig. 8E, F**). The support surface of C57Bl/6 mice gradually decreased with time, with a recovery of the static posture functions at 14 dpo ($P>0.05$ between pre-op and 14 dpo; **Fig. 8E**). Interestingly, Bral2 KO mice showed a faster vestibular compensation, as they returned to pre-operative values at 7 dpo ($P>0.05$ between pre-op and 7 dpo; **Fig. 8F**).

From these experiments we can conclude that i) Bral2 plays a crucial role for PNN function; ii) the presence of reduced PNNs in the vestibular nuclei promotes plasticity mechanisms underlying vestibular compensation.

Discussion

In this study we combined the evaluation of mouse behavioural changes following UL with the analysis of axonal plasticity and PNN modifications in the LVN. Our main findings were the following: i) recovery of vestibular static functions occurs in the second week after UL, while compensation of dynamic functions occurs in the fourth week; ii) recovery of static reflexes is accompanied by an increased number of GABAergic boutons in the contralateral LVN (**Table I**); iii) compensation of dynamic reflexes is additionally accompanied by a dramatic increase in the number of glutamatergic terminals in the ipsilateral LVN and, to a lesser extent, in the contralateral LVN (**Table I**); iv) PNNs are strongly reduced in number and staining intensity during the course of vestibular compensation and are completely restored when dynamic vestibular deficits are resolved (**Table I**); v) in mice with genetically defective PNNs (Bral2 KO mice) functional recovery after UL is accelerated.

Structural plasticity in the LVN during vestibular compensation

We observed a progressive decrease in the number of glutamatergic terminals after UL in the ipsilateral LVN, which was particularly evident when looking at VGLUT1-positive boutons. Those terminals represent a subpopulation of VGLUT2-positive endings, which are usually endowed with large size. Accordingly, Gacek and Schoonmaker (1997) show that UL results in a progressive loss of vestibular axons mainly of the largest diameter, suggesting that distinct types of vestibular nerve fibres may have a different sensitivity to the mechanical lesion.

It is known that immediately following UL, ipsilateral VN neurons become silent, whereas the spontaneous discharge of contralateral vestibular neurons is increased. These events are thought to cause the severe oculomotor and postural symptoms that immediately follow the damage. Next, the imbalance between the resting discharges of neurons in the two VN disappears (Smith and Curthoys, 1989; Ris et al., 1995), in parallel with the amelioration of the static deficits (Vidal et al., 1998). The initial rapid stage of vestibular compensation is followed by a slower process in which the dynamic reflexes recover as well (Vibert et al., 1993; Gliddon et al., 2005). In this context, we can hypothesize that the increased number of GABAergic terminals in the contralateral LVN may contribute to the re-balancing of neural activity in the two VN at short time points after UL, which may underlie the recovery of static functions. The massive increase in VGLUT terminals in the denervated LVN, as well as in the contralateral LVN, together with the persistent increased GABAergic tone in the contralateral LVN may help the long-term restoration of balance in neuronal

activity between the two LVN, underlying the recovery of dynamic reflexes. These data are in agreement with previous studies reporting an increase in the number of synaptic profiles at long time points after UL in both LVN, particularly in the denervated side (Gacek and Schoonmaker, 1997). Those terminals are probably provided by sprouting afferents. In physiological conditions, VN neurons receive not only vestibular input from the ipsilateral labyrinth (Sotelo and Palay, 1970), but also visual inputs and somatosensory inputs (such as proprioceptive information from ocular, periocular, mandibular and neck regions through the primary trigeminal nerve or the sensory trigeminal complex neurons). In addition, cortical areas sensitive to such inputs and cerebellar nuclei neurons send direct projections to the VN (Pfaller and Arvidsson, 1988; Cullen, 2012). Therefore, the reduction of the vestibular input in the ipsilateral LVN may be compensated for by other sensory inputs (Curthoys, 2000; Curthoys and Halmagyi, 1995; Lacour, 2006; Lacour et al., 1997). Cross-modal plasticity is, indeed, a common strategy operated by the nervous system to compensate for the injury-induced loss of a specific sensory modality (Newton et al., 2002; Hildebrandt et al., 2011; Van Brussel et al., 2011; Zeng et al., 2012). Nonetheless, we cannot exclude that the increased number of glutamatergic boutons in the LVN at 24 dpo is due to sprouting of VN afferents from other sources, such as the contralateral VN, inferior olive, reticular formation, solitary tract nucleus or area postrema (Dieringer and Precht, 1979; Diagne et al., 2006; Zhang et al., 2010; Hisano et al., 2002), which are involved in motor/autonomic functions.

Perineuronal changes in the LVN during vestibular compensation

Previous works showed that different conditions that elicit functional plasticity are accompanied by attenuation of PNNs. For example, exposure of adult rats to enhanced environmental stimulation induces a reduction of PNNs in the visual cortex, associated with a restoration of ocular dominance plasticity (Sale et al., 2007). Enriched environment also induces a conspicuous reduction of PNNs in the mouse cerebellar nuclei, in which significant axon remodelling of Purkinje cells and precerebellar axon occurs (Foscarin et al., 2011). In the latter condition, enriched environment reduces the synthesis of key PNN components and, simultaneously, enhances their enzymatic degradation (Foscarin et al., 2011). Furthermore, a substantial reduction in CSPG and semaphorin3A levels in the PNNs is observed in partially deafferented cerebellar nuclei, in which remarkable anatomical plasticity takes place (Carulli et al., 2013). Consistently, in the present study we observed a strong reduction of PNN number and intensity/thickness in the LVN in parallel with compensatory axonal remodelling. Nonetheless, PNN reduction at short time points after UL may affect synaptic plasticity. Indeed, enzymatic removal of hyaluronan-based pericellular matrix

increases extrasynaptic AMPA receptor diffusion and the exchange of synaptic receptors, modulating short-term synaptic plasticity (Frischknecht et al., 2009). Intriguingly, PNN number and staining intensity are restored in coincidence with the compensation of vestibular functions. PNN restoration may thus contribute to the stabilisation of the re-wired neuronal connections which may underlie behavioural recovery. Therefore, we can conclude that during injury-induced compensatory processes PNNs are highly modifiable structures, and the content of PNN growth-regulatory cues may be actively modulated to facilitate or restrict structural plasticity according to specific functional requirements.

The mechanisms which regulate the expression and turnover of PNN components have not been completely elucidated. CSPGs of the lectican family (aggrecan, neurocan, brevican and versican) are proteolytically processed by a large number of proteases, such as matrix metalloproteases and a subset of a disintegrin and metalloproteinases with thrombospondin repeats (ADAMTS1, -4, -5, -8, -9, and -15; Abbaszade et al., 1999; Tortorella et al., 1999; Nakamura et al., 2000; Tang, 2001; Muir et al., 2002; Porter et al., 2005; Zimmermann and Dours-Zimmermann, 2008). Interestingly, the extracellular matrix can be remodelled by ADAMTS in conditions of homeostatic plasticity, in which destabilizing influences such as attenuation of excitation can be counterbalanced by presynaptic and/or postsynaptic mechanisms to preserve network stability. Indeed, long-term inactivation of neuronal networks has been shown to induce an increase in ADAMTS4-dependent brevican processing at synaptic sites, which may be a prerequisite for synaptic rearrangements (Valenzuela et al., 2014). In general, ADAMTSs, separating the hyaluronan-binding N-terminal domain from the C-terminals domain of the CSPGs, would remove a substantial part of the CS moieties (which are mainly growth-inhibitory) from the neuronal surface and overall alter the fine structure of the PNN. Hence, in the model of vestibular compensation, it will be interesting to study whether specific matrix degrading enzymes remove PNN growth-inhibitory cues, thereby allowing for local plastic changes. Understanding how PNNs are modulated is important in order to identify a new range of therapeutic possibilities for the enhancement of CNS plasticity and functional recovery after damage.

Finally, the present work demonstrates that PNN reduction is crucial for vestibular compensation, as mice with genetically defective PNNs (Bral2 KO mice) show accelerated functional recovery. Notably, these data highlight a key contribution of the link protein Bral2 for PNN function. Link proteins are a group of proteins that stabilize the binding between CSPGs and hyaluronic acid, therefore contributing to the assembly of the condensed matrix structure of the net. Cartilage link protein-1 and Bral-2 are two link proteins found in PNNs (Bekku et al., 2003; Rauch et al., 2004;

Carulli et al., 2006, 2007; Galtrey et al., 2008). The absence of link protein-1 in PNN-bearing cells *in vitro* prevents the formation of a compact surface pericellular matrix (Kwok et al., 2010). Knockout mice for link protein-1 exhibit attenuated PNNs throughout the nervous system and are endowed with persistent plasticity into adulthood (Carulli et al., 2010). In mice lacking Bral2, PNNs appear reduced in several hindbrain areas and display a strongly diminished brevican staining (Bekku et al., 2012). Importantly, for the first time, here we show that in the absence of Bral2, adult CNS plasticity is enhanced. These results may have important implications in view of clinical strategies not only to improve vestibular compensation in patients who do not recover completely after a unilateral vestibular damage, but also to enhance functional recovery after other types of nervous system injury.

Conclusions

In conclusion, in this study we show that functional recovery after vestibular injury depend on PNN changes in central structures. PNN decrease may contribute to the re-opening of a "critical period", in which substantial axonal remodelling takes place leading to the recovery of vestibular functions.

Ackowledgements

This work was supported by MIUR ex 60% and and PRIN 20107MSMA4 Grants (to D.C. and F.R.) and a Grant-in-Aid for Scientific Research on Innovative Areas (Grant No. 24110509 and No. 26110713) from the Ministry of Education, Culture, Sports, Science, and Technology (MEXT) of Japan (to T.O.).

References

Abbaszade, I., Liu, R.Q., Yang, F., Rosenfeld, S.A., Ross, O.H., Link, J.R., Ellis, D.M., Tortorella, M.D., Pratta, M.A., Hollis, J.M., Wynn, R., Duke, J.L., George, H.J., Hillman, M.C. Jr, Murphy, K., Wiswall, B.H., Copeland, R.A., Decicco, C.P., Bruckner, R., Nagase, H., Itoh, Y., Newton, R.C., Magolda, R.L., Trzaskos, J.M., Burn, T.C., 1999. Cloning and characterization of ADAMTS11, an aggrecanase from the ADAMTS family. J. Biol. Chem. 274, 23443-23450.

Balaban, C.D., Schuerger, R.J., Porter, J.D., 2000. Zonal organization of flocculo-vestibular connections in rats. Neuroscience 99, 669-682.

Bekku, Y., Su, W.D., Hirakawa, S., Fässler, R., Ohtsuka, A., Kang, J.S., Sanders, J., Murakami, T., Ninomiya, Y., Oohashi, T., 2003. Molecular cloning of Bral2, a novel brain-specific link protein, and immunohistochemical colocalization with brevican in perineuronal nets. Mol. Cell. Neurosci. 24, 148-159.

Bekku, Y., Saito, M., Moser, M., Fuchigami, M., Maehara, A., Nakayama, M., Kusachi, S., Ninomiya, Y., Oohashi T., 2012. Bral2 is indispensable for the proper localization of brevican and the structural integrity of the perineuronal net in the brainstem and cerebellum. J. Comp. Neurol. 520, 1721-1736.

Bouchard, M., Grote, D., Craven, S.E., Sun, Q., Steinlein, P., Busslinger, M., 2005. Identification of Pax2-regulated genes by expression profiling of the mid-hindbrain organizer region. Development 132, 2633-2643.

Brückner, G., Grosche, J., Schmidt, S., Härtig, W., Margolis, R.U., Delpech, B., Seidenbecher, C.I., Czaniera, R., Schachner, M., 2000. Postnatal development of perineuronal nets in wild-type mice and in a mutant deficient in tenascin-R. J. Comp. Neurol. 428, 616-629.

Campos Torres, A., Vidal, P.P., de Waele, C., 1999. Evidence for a microglial reaction within the vestibular and cochlear nuclei following inner ear lesion in the rat. Neuroscience 92, 1475-1490.

Campos-Torres, A., Touret, M., Vidal, P.P., Barnum, S., de Waele, C., 2005. The differential response of astrocytes within the vestibular and cochlear nuclei following unilateral labyrinthectomy or vestibular afferent activity blockade by transtympanic tetrodotoxin injection in the rat. Neuroscience 130, 853-865.

Carmichael, S.T., Archibeque, I., Luke, L., Nolan, T., Momiy, J., Li, S., 2005. Growth-associated gene expression after stroke: evidence for a growth-promoting region in peri-infarct cortex. Exp. Neurol. 193, 291-311.

Carulli, D., Rhodes, K.E., Brown, D.J., Bonnert, T.P., Pollack, S.J., Oliver, K., Strata, P., Fawcett, J.W., 2006. Composition of perineuronal nets in the adult rat cerebellum and the cellular origin of their components. J. Comp. Neurol. 494, 559-577.

Carulli, D., Rhodes, K.E., Fawcett, J.W., 2007. Upregulation of aggrecan, link protein 1, and hyaluronan synthases during formation of perineuronal nets in the rat cerebellum. J. Comp. Neurol. 501, 83-94.

Carulli, D., Pizzorusso, T., Kwok, J.C., Putignano, E., Poli, A., Forostyak, S., Andrews, M.R., Deepa, S.S., Glant, T.T., Fawcett, J.W., 2010. Animals lacking link protein have attenuated perineuronal nets and persistent plasticity. Brain 133, 2331-2347.

Carulli, D., Foscarin, S., Faralli, A., Pajaj, E., Rossi, F., 2013. Modulation of semaphorin3A in perineuronal nets during structural plasticity in the adult cerebellum. Mol. Cell. Neurosci. 57, 10-22.

Cullen, K.E., 2012. The vestibular system: multimodal integration and encoding of self-motion for motor control. Trends Neurosci. 35, 185-196.

Curthoys, I.S., Halmagyi, G.M., 1995. Vestibular compensation: a review of the oculomotor, neural, and clinical consequences of unilateral vestibular loss. J. Vestib. Res. 5, 67-107.

Curthoys, I.S., Halmagyi, G.M., 1999. Vestibular compensation. Adv. Otorhinolaryngol. 55, 82-110.

Curthoys, I.S., 2000. Vestibular compensation and substitution. Curr. Opin. Neurol. 13, 27-30.
de Waele, C., Campos Torres, A., Josset, P., Vidal, P.P., 1996. Evidence for reactive astrocytes in rat vestibular and cochlear nuclei following unilateral inner ear lesion. Eur. J. Neurosci. 8, 2006-2018.
Deák, Á., Bácskai, T., Gaál, B., Rácz, É., Matesz, K., 2012. Effect of unilateral labyrinthectomy on the molecular composition of perineuronal nets in the lateral vestibular nucleus of the rat. Neurosci. Lett. 513, 1-5.
Diagne, M., Valla, J., Delfini, C., Buisseret-Delmas, C., Buisseret, P., 2006. Trigeminovestibular and trigeminospinal pathways in rats: retrograde tracing compared with glutamic acid decarboxylase and glutamate immunohistochemistry. J. Comp. Neurol. 496, 759-772.
Dieringer, N., Precht, W., 1979. Synaptic mechanisms involved in compensation of vestibular function following hemilabyrinthectomy. Prog. Brain Res. 50, 607-615.
Dutheil, S., Brezun, J.M., Leonard, J., Lacour, M., Tighilet, B., 2009. Neurogenesis and astrogenesis contribution to recovery of vestibular functions in the adult cat following unilateral vestibular neurectomy: cellular and behavioral evidence. Neuroscience 164, 1444-1456.
Dutheil, S., Escoffier, G., Gharbi, A., Watabe, I., Tighilet, B., 2013. GABA(A) receptor agonist and antagonist alter vestibular compensation and different steps of reactive neurogenesis in deafferented vestibular nuclei of adult cats. J Neurosci. 33, 15555-15566.
Foscarin, S., Rossi, F., Carulli, D., 2012. Influence of the environment on adult CNS plasticity and repair. Cell Tissue Res. 349, 161-167.
Frischknecht, R., Heine, M., Perrais, D., Seidenbecher, C.I., Choquet, D., Gundelfinger, E.D., 2009. Brain extracellular matrix affects AMPA receptor lateral mobility and short-term synaptic plasticity. Nat. Neurosci. 12, 897-904.
Gacek, R.R., Schoonmaker, J.E., 1997. Morphologic changes in the vestibular nerves and nuclei after labyrinthectomy in the cat: a case for the neurotrophin hypothesis in vestibular compensation. Acta Otolaryngol. 117, 244-249.
Galtrey, C.M., Kwok, J.C., Carulli, D., Rhodes, K.E., Fawcett, J.W., 2008. Distribution and synthesis of extracellular matrix proteoglycans, hyaluronan, link proteins and tenascin-R in the rat spinal cord. Eur. J. Neurosci. 27, 1373-1390.
Geissler, M., Gottschling, C., Aguado, A., Rauch, U., Wetzel, C.H., Hatt, H., Faissner, A., 2013. Primary hippocampal neurons, which lack four crucial extracellular matrix molecules, display abnormalities of synaptic structure and function and severe deficits in perineuronal net formation. J. Neurosci. 33, 7742-7755.
Gliddon, C.M., Darlington, C.L., Smith, P.F., 2005. GABAergic systems in the vestibular nucleus and their contribution to vestibular compensation. Prog. Neurobiol. 75, 53-81.
Gogolla, N., Caroni, P., Lüthi, A., Herry, C., 2009. Perineuronal nets protect fear memories from erasure. Science 325, 1258-1261.
Grassi, S., Pettorossi, V.E., 2001. Synaptic plasticity in the medial vestibular nuclei: role of glutamate receptors and retrograde messengers in rat brainstem slices. Prog. Neurobiol. 64, 527-553.
Gustave Dit Duflo, S., Gestreau, C., Tighilet, B., Lacour, M., 1999. Fos expression in the cat brainstem after unilateral vestibular neurectomy. Brain Res. 824, 1-17.
Happel, M.F., Niekisch, H., Castiblanco Rivera, L.L., Ohl, F.W., Deliano, M., Frischknecht, R., 2014. Enhanced cognitive flexibility in reversal learning induced by removal of the extracellular matrix in auditory cortex. Proc. Natl. Acad. Sci. U. S. A. 111, 2800-2805.
Härtig, W., Brauer, K., Brückner, G., 1992. Wisteria floribunda agglutinin-labelled nets surround parvalbumin-containing neurons. Neuroreport 3, 869-72.
Highstein, S.M., McCrea, R.A., 1988. The anatomy of the vestibular nuclei. Rev. Oculomot. Res. 2, 177-202.

Hildebrandt, H., Hoffmann, N.A., Illing, R.B., 2011. Synaptic reorganization in the adult rat's ventral cochlear nucleus following its total sensory deafferentation. PLoS One 6, e23686.

Hisano, S., Sawada, K., Kawano, M., Kanemoto, M., Xiong, G., Mogi, K., Sakata-Haga, H., Takeda, J., Fukui, Y., Nogami, H., 2002. Expression of inorganic phosphate/vesicular glutamate transporters (BNPI/VGLUT1 and DNPI/VGLUT2) in the cerebellum and precerebellar nuclei of the rat. Brain Res. Mol. Brain Res. 107, 23-31.

Holstein, G.R., Martinelli, G.P., Cohen, B., 1999. Ultrastructural features of non-commissural GABAergic neurons in the medial vestibular nucleus of the monkey. Neuroscience 93, 183-93.

Köppe, G., Brückner, G., Brauer, K., Härtig, W., Bigl, V., 1997. Developmental patterns of proteoglycan-containing extracellular matrix in perineuronal nets and neuropil of the postnatal rat brain. Cell Tissue Res. 288, 33-41.

Kwok, J.C., Carulli, D., Fawcett, J.W., 2010. In vitro modeling of perineuronal nets: hyaluronan synthase and link protein are necessary for their formation and integrity. J. Neurochem. 114, 1447-1459.

Kwok, J.C., Dick, G., Wang, D., Fawcett, J.W., 2011. Extracellular matrix and perineuronal nets in CNS repair. Dev. Neurobiol. 71, 1073-1089.

Lacour, M., Tighilet, B., 2010. Plastic events in the vestibular nuclei during vestibular compensation: the brain orchestration of a "deafferentation" code. Restor. Neurol. Neurosci. 28, 19-35.

Lacour, M., Barthelemy, J., Borel, L., Magnan, J., Xerri, C., Chays, A., Ouaknine, M., 1997. Sensory strategies in human postural control before and after unilateral vestibular neurotomy. Exp. Brain Res. 115, 300-310.

Lacour, M., Dutheil, S., Tighilet, B., Lopez, C., Borel, L., 2009. Tell me your vestibular deficit, and i'll tell you how you'll compensate. Ann. N. Y. Acad. Sci. 1164, 268-278.

Lacour, M., 2006. Restoration of vestibular function: basic aspects and practical advances for rehabilitation. Curr. Med. Res. Opin. 22, 1651-1659.

Li, H., Dokas, L.A., Godfrey, D.A., Rubin, A.M., 2002-2003. Remodeling of synaptic connections in the deafferented vestibular nuclear complex. J. Vestib. Res. 12, 167-183.

Liberge, M., Manrique, C., Bernard-Demanze, L., Lacour, M., 2010. Changes in TNFα, NFκB and MnSOD protein in the vestibular nuclei after unilateral vestibular deafferentation. J. Neuroinflammation 7, 91.

Muir, E.M., Adcock, K.H., Morgenstern, D.A., Clayton, R., von Stillfried, N., Rhodes, K., Ellis, C., Fawcett, J.W., Rogers, J.H., 2002. Matrix metalloproteases and their inhibitors are produced by overlapping populations of activated astrocytes. Brain Res. Mol. Brain Res. 100, 103-117.

Nakamura, H., Fujii, Y., Inoki, I., Sugimoto, K., Tanzawa, K., Matsuki, H., Miura, R., Yamaguchi, Y., Okada, Y., 2000. Brevican is degraded by matrix metalloproteinases and aggrecanase-1 (ADAMTS4) at different sites. J. Biol. Chem. 275, 38885-38890.

Newton, J.R., Sikes, R.W., Skavenski, A.A., 2002. Cross-modal plasticity after monocular enucleation of the adult rabbit. Exp. Brain Res. 144, 423-429.

Pfaller, K., Arvidsson, J., 1988. Central distribution of trigeminal and upper cervical primary afferents in the rat studied by anterograde transport of horseradish peroxidase conjugated to wheat germ agglutinin. J. Comp. Neurol. 268, 91-108.

Pizzorusso, T., Medini, P., Berardi, N., Chierzi, S., Fawcett, J.W., Maffei, L., 2002. Reactivation of ocular dominance plasticity in the adult visual cortex. Science 298, 1248-1251.

Pizzorusso, T., Medini, P., Landi, S., Baldini, S., Berardi, N., Maffei, L., 2006. Structural and functional recovery from early monocular deprivation in adult rats. Proc. Natl. Acad. Sci. U. S. A. 103, 8517-8522.

Porter, S., Clark, I.M., Kevorkian, L., Edwards, D.R., 2005. The ADAMTS metalloproteinases. Biochem. J. 386, 15-27.

Rácz, E., Gaál, B., Kecskes, S., Matesz, C., 2014. Molecular composition of extracellular matrix in the vestibular nuclei of the rat. Brain Struct. Funct. 219, 1385-1403.
Rauch, U., 2004. Extracellular matrix components associated with remodeling processes in brain. Cell. Mol. Life Sci. 61, 2031-2045.
Ris, L., de Waele, C., Serafin, M., Vidal, P.P., Godaux, E., 1995. Neuronal activity in the ipsilateral vestibular nucleus following unilateral labyrinthectomy in the alert guinea pig. J. Neurophysiol. 74, 2087-2099.
Romberg, C., Yang, S., Melani, R., Andrews, M.R., Horner, A.E., Spillantini, M.G., Bussey, T.J., Fawcett, J.W., Pizzorusso, T., Saksida, L.M., 2013. Depletion of perineuronal nets enhances recognition memory and long-term depression in the perirhinal cortex. J. Neurosci. 33, 7057-7065.
Sale, A., Maya Vetencourt, J.F., Medini, P., Cenni, M.C., Baroncelli, L., De Pasquale, R., Maffei, L., 2007. Environmental enrichment in adulthood promotes amblyopia recovery through a reduction of intracortical inhibition. Nat. Neurosci. 10, 679-681.
Smith, P.F., Curthoys, I.S., 1989. Mechanisms of recovery following unilateral labyrinthectomy: a review. Brain Res. Brain Res. Rev. 14, 155-180.
Smith, P.F., Darlington, C.L., Yan, Q., Dragunow, M., 1998. Unilateral vestibular deafferentation induces brain-derived neurotrophic factor (BDNF) protein expression in the guinea pig lateral but not medial vestibular nuclei. J. Vestib. Res. 8, 443-447.
Sotelo, C., Palay, S.L., 1970. The fine structure of the later vestibular nucleus in the rat. II. Synaptic organization. Brain Res. 18, 93-115.
Tang, B.L., 2001. ADAMTS: a novel family of extracellular matrix proteases. Int. J. Biochem. Cell Biol. 33, 33-44.
Tighilet, B., Lacour, M., 2001. Gamma amino butyric acid (GABA) immunoreactivity in the vestibular nuclei of normal and unilateral vestibular neurectomized cats. Eur. J. Neurosci. 13, 2255-2267.
Tighilet, B., Lacour, M., 1998. Distribution of choline acetyltransferase immunoreactivity in the vestibular nuclei of normal and unilateral vestibular neurectomized cats. Eur. J. Neurosci. 10, 3115-3126.
Tighilet, B., Brezun, J.M., Sylvie, G.D., Gaubert, C., Lacour, M., 2007. New neurons in the vestibular nuclei complex after unilateral vestibular neurectomy in the adult cat. Eur. J. Neurosci. 25, 47-58.
Tortorella, M.D., Burn, T.C., Pratta, M.A., Abbaszade, I., Hollis, J.M., Liu, R., Rosenfeld, S.A., Copeland, R.A., Decicco, C.P., Wynn, R., Rockwell, A., Yang, F., Duke, J.L., Solomon, K., George, H., Bruckner, R., Nagase, H., Itoh, Y., Ellis, D.M., Ross, H., Wiswall, B.H., Murphy, K., Hillman, M.C. Jr, Hollis, G.F., Newton, R.C., Magolda, R.L., Trzaskos, J.M., Arner, E.C., 1999. Purification and cloning of aggrecanase-1: a member of the ADAMTS family of proteins. Science 284, 1664-1666.
Valenzuela, J.C., Heise, C., Franken, G., Singh, J., Schweitzer, B., Seidenbecher, C.I., Frischknecht, R., 2014. Hyaluronan-based extracellular matrix under conditions of homeostatic plasticity. Philos. Trans. R. Soc. Lond. B. Biol. Sci. 369, 20130606.
Van Brussel, L., Gerits, A., Arckens, L, 2011. Evidence for cross-modal plasticity in adult mouse visual cortex following monocular enucleation. Cereb. Cortex 21, 2133-2146.
Vibert, N., de Waele, C., Escudero, M., Vidal, P.P., 1993. The horizontal vestibulo-ocular reflex in the hemilabyrinthectomized guinea-pig. Exp. Brain Res. 97, 263-273.
Vidal, P.P., de Waele, C., Vibert, N., Mühlethaler, M., 1998. Vestibular compensation revisited. Otolaryngol. Head Neck Surg. 119, 34-42.
Vo, T., Carulli, D., Ehlert, E.M., Kwok, J.C., Dick, G., Mecollari, V., Moloney, E.B., Neufeld, G., de Winter, F., Fawcett, J.W., Verhaagen, J., 2013. The chemorepulsive axon guidance protein

semaphorin3A is a constituent of perineuronal nets in the adult rodent brain. Mol. Cell. Neurosci. 56, 186-200.

Wang, D., Fawcett, J.W., 2012. The perineuronal net and the control of CNS plasticity. Cell Tissue Res. 349, 147-160.

Yang, S., Cacquevel, M., Saksida, L.M., Bussey, T.J., Schneider, B.L., Aebischer, P., Melani, R., Pizzorusso, T., Fawcett, J.W., Spillantini, M.G., 2014. Perineuronal net digestion with chondroitinase restores memory in mice with tau pathology. Exp. Neurol. pii: S0014-4886(14)00383-5.

Zeng, C., Yang, Z., Shreve, L., Bledsoe, S., Shore, S., 2012. Somatosensory projections to cochlear nucleus are upregulated after unilateral deafness. J. Neurosci. 32, 15791-15801.

Zhang, F.X., Pang, Y.W., Zhang, M.M., Zhang, T., Dong, Y.L., Lai, C.H., Shum, D.K., Chan, Y.S., Li, J.L., Li, Y.Q., 2011. Expression of vesicular glutamate transporters in peripheral vestibular structures and vestibular nuclear complex of rat. Neuroscience 173, 179-189.

Zimmermann, D.R., Dours-Zimmermann, M.T., 2008. Extracellular matrix of the central nervous system: from neglect to challenge. Histochem. Cell Biol. 130, 635-653.

Figure legends

Figure 1. Recovery of vestibular static and dynamic reflexes after UL in FVB mice. A. Mean value (in cm^2 ± SEM) of the support surface of the mice (n = 6) evaluated before UL and at different time points after UL (days post-operation, dpo). Note the strong increase in the support surface at 1 dpo and the progressive decrease afterwards, with a complete recovery at 12 dpo (one-way ANOVA on repeated measures, Dunnett's post-hoc test for comparison of each time point with pre-op value). **B** shows the global score of the mice (n = 6) in the air-righting and landing reflex tests (± SEM) before UL and at different time points after UL (days post-operation, dpo). A "0" score indicates normal dynamic reflexes, scores between 1 and 4 indicate compromised reflexes. Vestibular dynamic deficits improve with time and recover at 24 dpo (one-way ANOVA on repeated measures, Dunnett's post-hoc test for comparison of each time point with pre-op values). ** P<0.01, *** P<0.001

Figure 2. Glutamatergic axon terminals in the intact LVN. A. Immunofluorescence for VGLUT1 (green) and VGLUT2 (red) shows that the majority of glutamatergic terminals in the LVN are VGLUT2-positive/VGLUT1-negative, a small fraction of VGLUT2-positive terminals also express VGLUT1 (arrows), and very few terminals express VGLUT1 only (arrowhead). **B**. Percentage of VGLUT1, VGLUT2 and VGLUT1/VGLUT2 boutons. **C.** Glutamatergic terminals immunoreactive for VGLUT1 have a larger size than VGLUT2-positive terminals (T-test, P<0.001), which include VGLUT2-only and VGLUT1/VGLUT2-terminals. Scale bar: 10 µm.

Figure 3. Axonal plasticity in the denervated (ipsilateral) LVN. A-E. VGLUT1-terminals (green) are decreased in number at 3, 6 and 12 dpo and strongly increased at 24 dpo in the denervated LVN. **F-J** show that the density of VGLUT2-positive boutons (red) is decreased at 3, 6 and 12 dpo, and returns to control levels at 24 dpo. **K-O.** Immunoreactivity for VGAT (red) shows that GABAergic terminals do not change in number after UL in the denervated LVN. **P.** Quantification of the density of VGLUT1 boutons at different time points after UL. **Q**. Quantification of the density of VGLUT2-terminals. **R**. Quantification of the density of VGAT-positive terminals. * P<0.05, ** P<0.01, *** P<0.001. Scale bars: 15 µm in A (also applies to B-O).

Figure 4. Axonal plasticity in the intact (contralateral) LVN. A-E. The density of VGLUT1-terminals (green) in the contralateral LVN does not substantially change at short time after UL but increase at 24 dpo. **F-J**. The density of VGLUT2-positive terminals (red) in the intact LVN does not change after UL. **K-O.** The density of VGAT-positive terminals (red) is increased in the

contralateral LVN during vestibular compensation, particularly at 6, 12 and 24 dpo. In (**P**), quantification of the density of VGLUT1-terminals in the intact LVN **Q.** Quantification of the density of VGLUT2-positive terminals. **R.** Quantification of the density of VGAT-terminals. *** P < 0.001. Scale bars: 15 µm in A (also applies to B-O).

Figure 5. Distribution pattern of PNNs in the LVN. PNNs, visualized by WFA reactivity (red), are found mainly around SMI32-positive neurons (blue), i.e projection neurons (Campbell and Morrison, 1989) (**A-D**). **E.** Virtually all SMI32-positive neurons possess a PNN; approximately 60% of them are glutamatergic (arrow in A-C), 40% of them GABAergic (arrowheads in A-C), according to their GFP expression (green) in Pax2-GFP mice. **F.** Among GABAergic neurons, approximately 60% of them bear a PNN, 1/3 of those being local interneurons (SMI32-negative, asterisk in A-C) and 2/3 projection neurons (SMI32+). Scale bar: 30 µm.

Figure 6. PNN expression in the denervated LVN during vestibular compensation. Both the number of neurons bearing a WFA-positive PNN and WFA staining intensity are strongly reduced in the ispilateral LVN at short time points after UL (**A-C'**). At 12 dpo the number of the nets return to control levels, although their intensity is still low (**D, D'**). At 24 dpo both the number and the intensity of PNNs are restored (**E, E'**). **F**. Quantification of the percentage of neurons bearing a PNN in the denervated LVN at different time points after UL (One-way ANOVA, Dunnett's post-hoc test). **G**. Frequency distribution of PNNs subdivided in three categories according to their WFA staining intensity (see methods; X^2-test). Neurons are stained by NeuN antibodies (green) and PNNs by WFA histochemistry (red). *** P < 0.001. Scale bar: 20 µm in A (also applies to A'-E').

Figure 7. PNN expression in the intact LVN during vestibular compensation. Both the number of neurons bearing a WFA-positive PNN and WFA staining intensity are slightly reduced in the ispilateral LVN at 3 dpo (**A-B'**). The number of PNNs is restored from 3 dpo (**C-E**), while WFA staining intensity remains low at 6 and 12 dpo (**C-D'**) and returns to control levels at 24 dpo (**E, E'**). **F**. Quantification of the percentage of neurons bearing a PNN in the contralateral LVN at different time points after UL (One-way ANOVA, Dunnett's post-hoc test). **G**. Frequency distribution of PNNs subdivided in three categories according to their WFA staining intensity (X^2-test). Neurons are stained by NeuN antibodies (green) and PNNs by WFA histochemistry (red). *** P < 0.001. Scale bar: 20 µm in A (also applies to A'-E').

Figure 8. Bral2 KO mice show attenuated PNNs in the LVN and faster vestibular compensation. Both WFA histochemistry (red in **A, B**) and brevican immunoreactivity (green in **C,**

D) are strongly attenuated in the LVN of adult Bral2 KO mice when compared to WT mice. **E, F**. Support surface (expressed as a percentage increase from pre-op values) of C57Bl/6 (n = 11; **E**) and Bral2 KO mice (n = 15; **F**) at different time points after UL. Compensation of vestibular deficits occurs at 14 dpo in WT mice and at 7 dpo in the KOs (One-way ANOVA on repeated measures, Dunnett's post-hoc). ** P<0.01, *** P<0.001. Scale bar: 25 µm in A and C (also applies to B and D).

Supplementary figure legend 1. The average size of VGLUT2-positive terminals is decreased at 12 dpo in the ispilateral LVN. A, B. Representative pictures of VGLUT2-positive terminals in the LVN of a control animal (A) and in the ispilateral LVN of a UL-animal at 12 dpo (B). In (**C**), quantification of the size of VGLUT2-boutons. *** P<0.001. Scale bar: 5 µm in A (also applies to B).

Supplementary figure legend 2. Morphology of the PNNs in the denervated LVN at 3 day after UL. WFA-bearing PNNs show a disorganised appearance and decreased thickness in the denervated LVN at 3 dpo (**B**) when compared to PNNs in the LVN of control animals (**A**). Scale bar: 25 µm in A (also applies to B).

Table I. Anatomical plasticity in the LVN after UL in parallel with behavioural changes.

	3 dpo		6 dpo		12 dpo		24 dpo	
Behaviour	Slight amelioration of static and dynamic deficits		Amelioration of static and dynamic deficits		Recovery of static deficits		Recovery of dynamic deficits	
	Denerv. LVN	**Intact LVN**	**Denerv. LVN**	**Intact LVN**	**Denerv. LVN**	**Intact LVN**	**Denerv. LVN**	**Intact LVN**
VGLUT1 density	↓↓	—	↓↓	—	↓↓↓	—	↑↑↑	↑↑
VGLUT2 density	↓↓	—	↓↓	—	↓↓	—	—	—
VGAT density	—	—	—	↑↑	—	↑↑	—	↑↑
PNN number	↓↓	↓	↓	—	—	—	—	—
PNN intensity	↓↓	↓	↓↓↓	↓↓	↓↓↓	↓	—	—

Denerv. = denervated; dpo = days post-operation; — = unchanged; ↓ = small decrease; ↓↓ = moderate decrease; ↓↓↓ = big decrease; ↑↑ = moderate increase; ↑↑↑ = big increase, with respect to control condition.

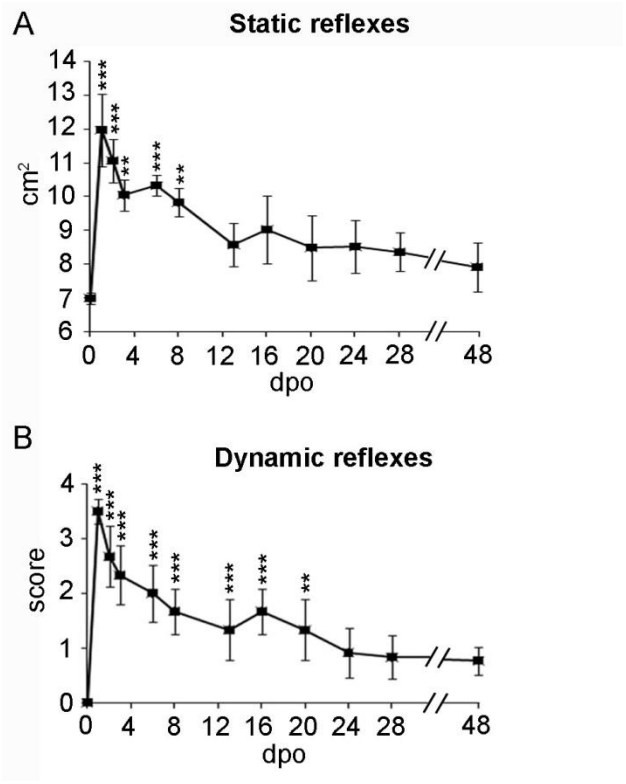

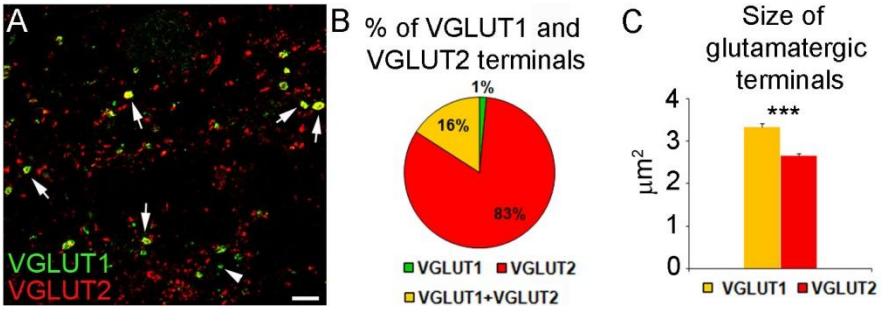
A
VGLUT1
VGLUT2
B
% of VGLUT1 and VGLUT2 terminals
1%
16%
83%
VGLUT1
VGLUT2
VGLUT1+VGLUT2
C
Size of glutamatergic terminals
***
µm²
4
3
2
1
0
VGLUT1
VGLUT2

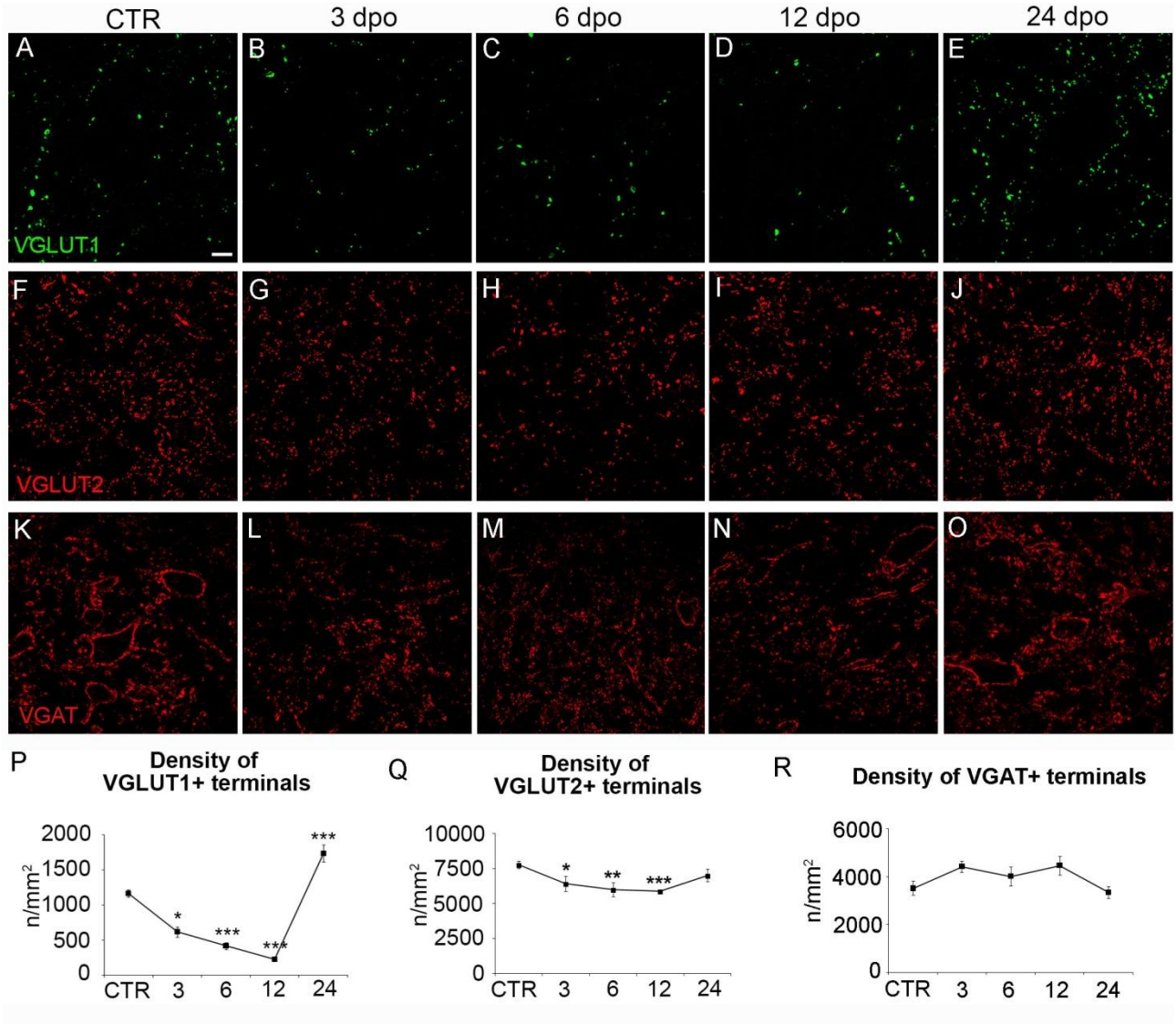
CTR
3 dpo
6 dpo
12 dpo
24 dpo
A
B
C
D
E
VGLUT1
F
G
H
I
J
VGLUT2
K
L
M
N
O
VGAT
P
Density of VGLUT1+ terminals
n/mm²
2000
1500
1000
500
0
CTR
3
6
12
24
Q
Density of VGLUT2+ terminals
10000
7500
5000
2500
0
R
Density of VGAT+ terminals
6000
4000
2000

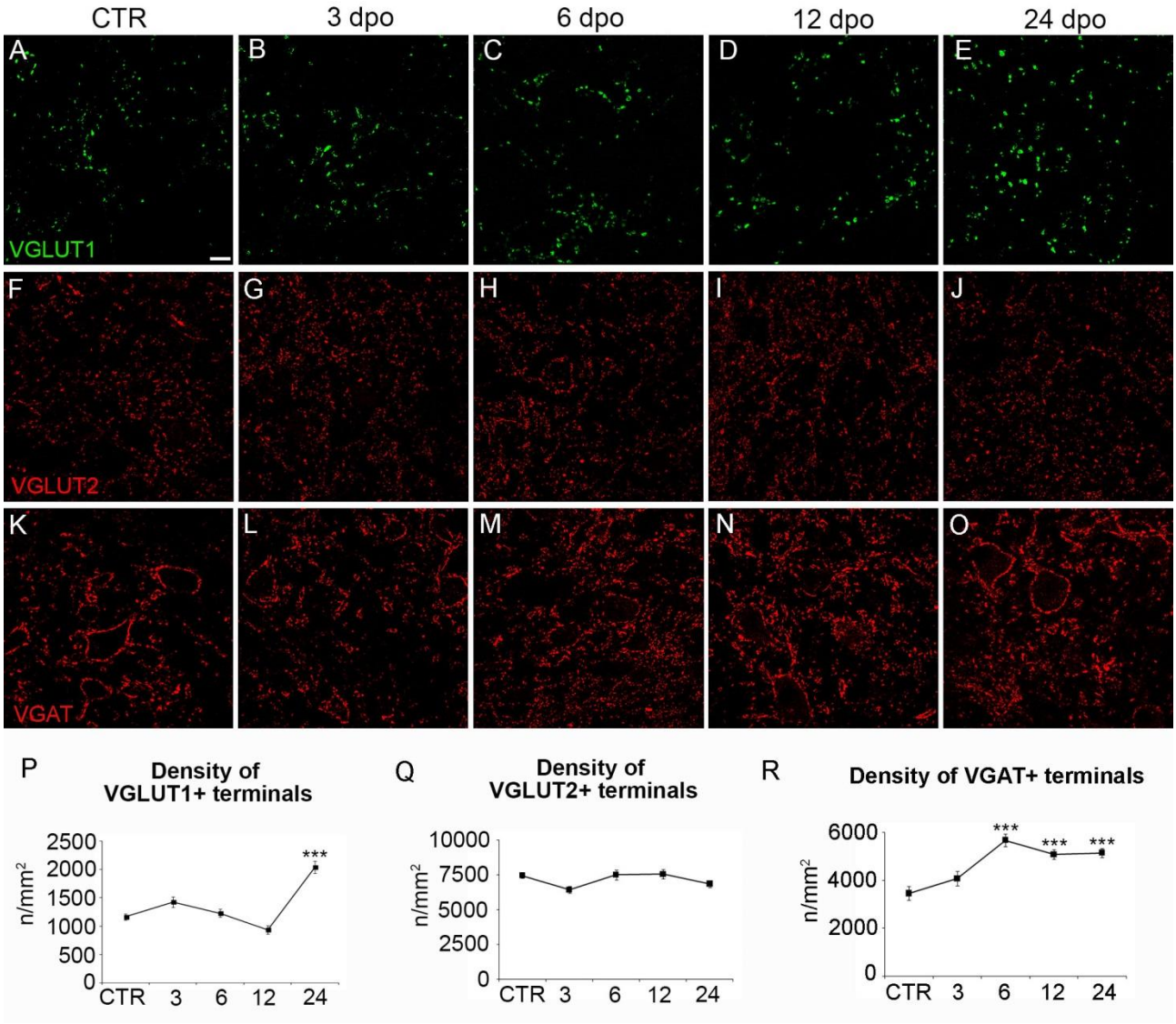
CTR
3 dpo
6 dpo
12 dpo
24 dpo
A
B
C
D
E
VGLUT1
F
G
H
I
J
VGLUT2
K
L
M
N
O
VGAT
P
Density of VGLUT1+ terminals
n/mm2
2500
2000
1500
1000
500
0
CTR 3 6 12 24
***
Q
Density of VGLUT2+ terminals
n/mm2
10000
7500
5000
2500
0
CTR 3 6 12 24
R
Density of VGAT+ terminals
n/mm2
6000
4000
2000
0
CTR 3 6 12 24
***
***
***

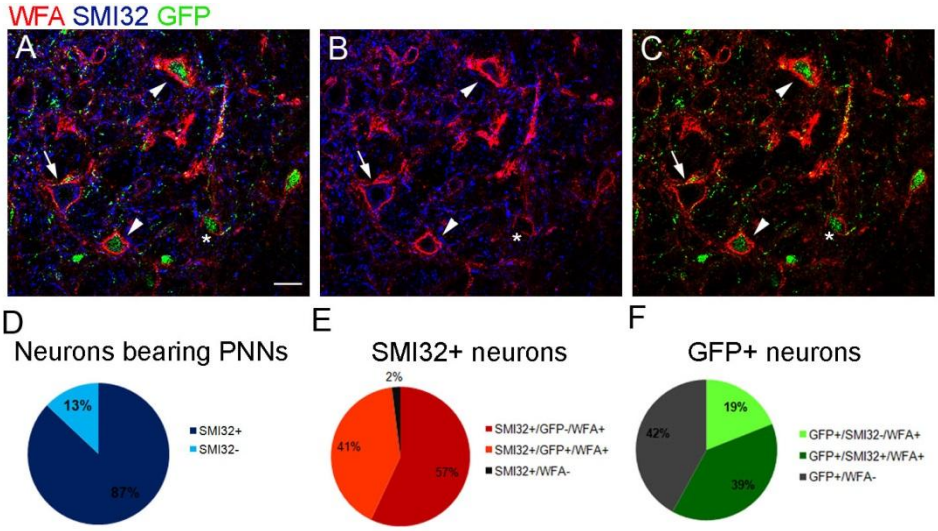
WFA SMI32 GFP
A
B
C
D
Neurons bearing PNNs
13%
87%
SMI32+
SMI32-
E
SMI32+ neurons
2%
41%
57%
SMI32+/GFP-/WFA+
SMI32+/GFP+/WFA+
SMI32+/WFA-
F
GFP+ neurons
19%
42%
39%
GFP+/SMI32-/WFA+
GFP+/SMI32+/WFA+
GFP+/WFA-

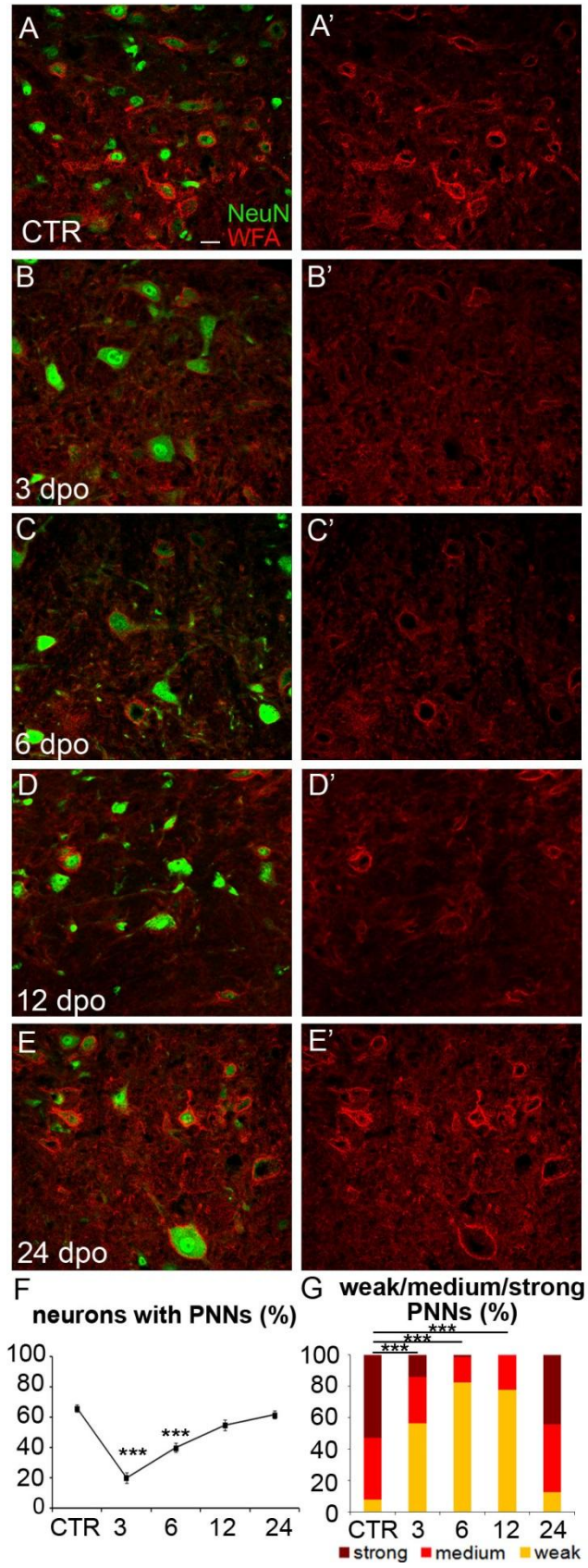
A
A'
CTR
NeuN
WFA
B
B'
3 dpo
C
C'
6 dpo
D
D'
12 dpo
E
E'
24 dpo
F
neurons with PNNs (%)
100
80
60
40
20
0
***
***
CTR 3 6 12 24
G
weak/medium/strong PNNs (%)
***
***
***
100
80
60
40
20
0
CTR 3 6 12 24
strong
medium
weak

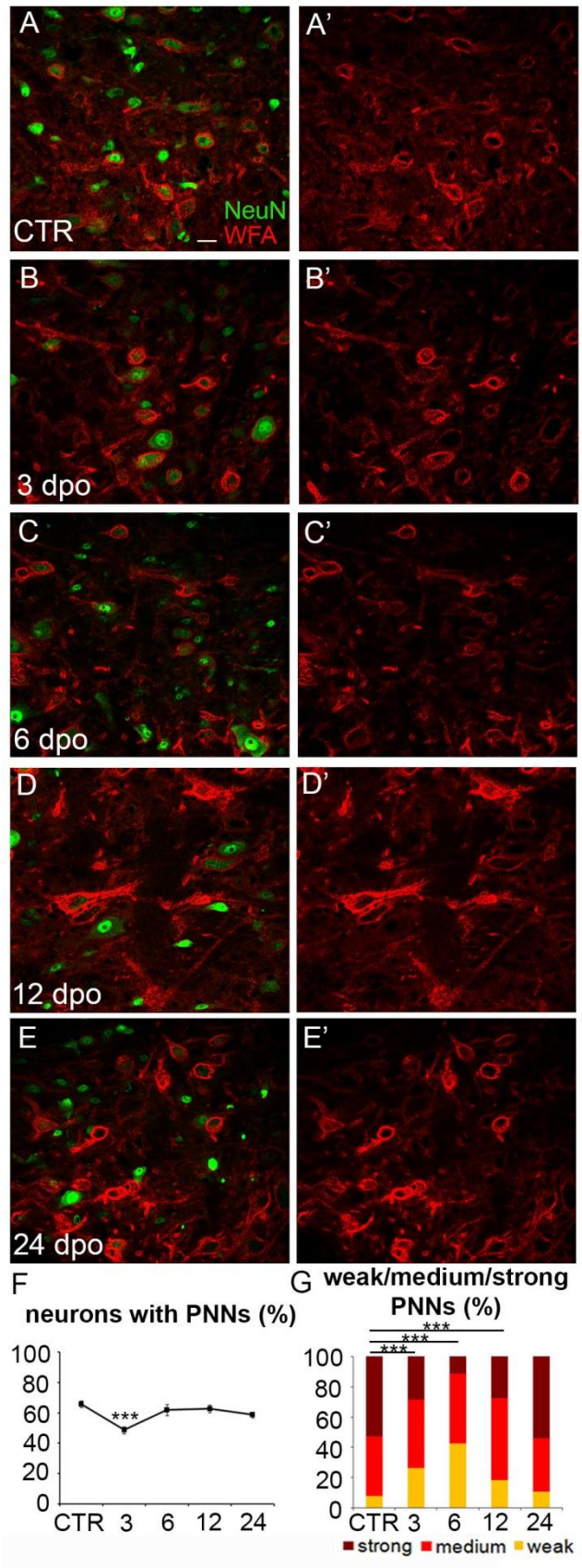
A
A'
CTR
NeuN
WFA
B
B'
3 dpo
C
C'
6 dpo
D
D'
12 dpo
E
E'
24 dpo
F
neurons with PNNs (%)
100
80
60
40
20
0
***
CTR 3 6 12 24
G
weak/medium/strong PNNs (%)
***
***
***
100
80
60
40
20
0
CTR 3 6 12 24
strong
medium
weak

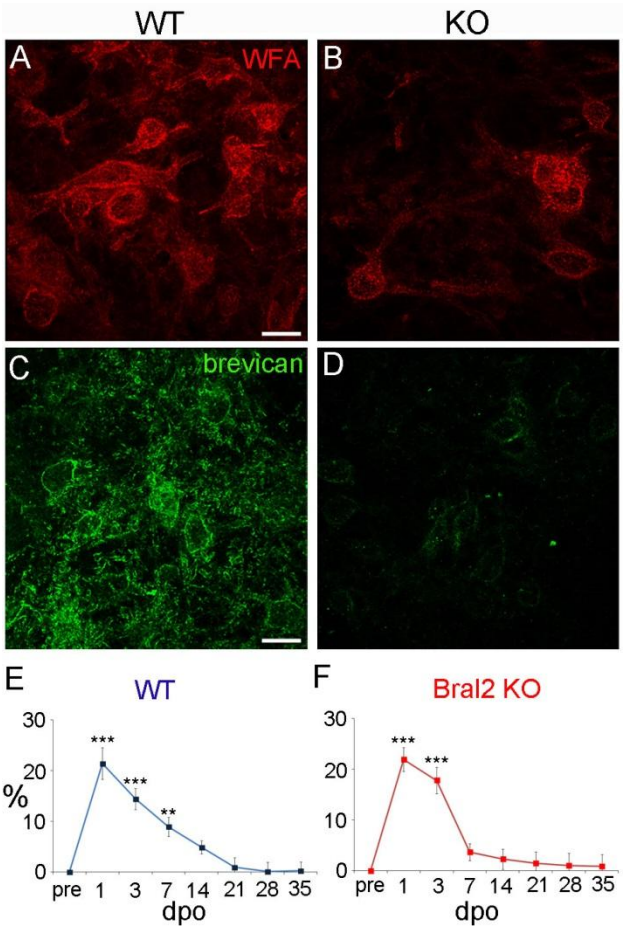
WT
KO
A
WFA
B
C
brevican
D
E
WT
F
Bral2 KO
30
20
10
0
%
***
**
pre 1 3 7 14 21 28 35
dpo

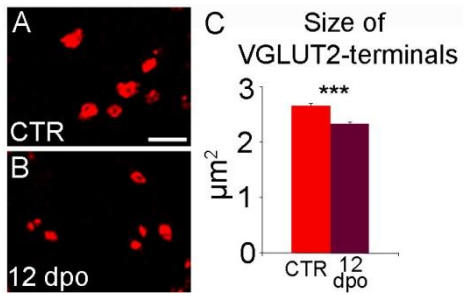
A
CTR
B
12 dpo
C
Size of
VGLUT2-terminals
3
2
1
0
µm²
***
CTR
12
dpo

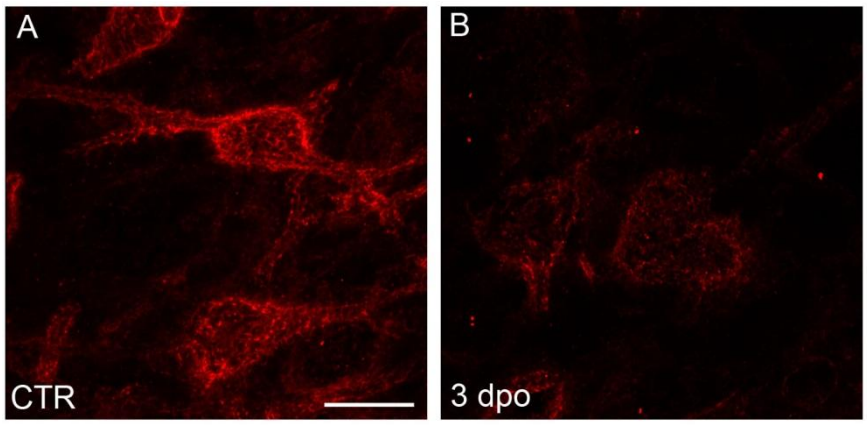
A
CTR
B
3 dpo